Structural information on Y ions in C_{82} from EXAFS experiments

C.-H. Park, B.O. Wells, J. DiCarlo, Z.-X. Shen
Department of Applied Physics and Stanford Synchrotron Radiation Laboratory, Stanford University, Stanford, CA 94305, USA

Jesse R. Salem, Donald S. Bethune, Costantino S. Yannoni,
Robert D. Johnson, Mattanjah S. de Vries
Almaden Research Center, IBM Research Division, 650 Harry Road, San Jose, CA 95120, USA

Corwin Booth, Frank Bridges
Physics Department, University of California, Santa Cruz, CA 95064, USA

and

Piero Pianetta
Stanford Synchrotron Radiation Laboratory, Stanford University, Stanford, CA 94305, USA

Received 16 July 1993

EXAFS experiments on a fullerene sample containing both YC_{82} and Y_2C_{82} are reported, performed both at 10 K and at room temperature, to probe the structural environment of the yttrium atoms. The results are similar at both temperatures. The data can be fit with a model with two shells of 6 carbon atoms each, at 2.4 and 2.9 Å, respectively. This result supports the hypothesis that the metal atoms are trapped inside the fullerene cage, consistent with recent calculations on possible metallofullerene structures.

1. Introduction

Experimental evidence for the existence of fullerene cages with atoms inside the cavity has generated intense interest, both because of potential new chemistry and because of potential new materials properties. The initial reports in 1985 contained only circumstantial evidence for the endohedral structures, since the macroscopic quantities of material required for traditional structural probes were not available [1]. So called "shrink wrapping" experiments [2], showed that photodissociation proceeds via successive loss of carbon pairs, rather than loss of the metal atom, until the carbon cage shrinks to approximately the size of the metal ion radius. XPS and EPR experiments have been reported on mixtures of C_{60} and C_{70} metallofullerenes containing one or more group IIIB metals [3–11]. In the monometal species, the metals are found to be in a 3^+ oxidation state. Recent theoretical calculations found a +3 valence for lanthanum at its optimal position *inside* the carbon shell, but a +2 valence for *external* positions [12,13]. EPR spectra of Sc_3C_{82} suggest that for that species all three Sc nuclei are equivalent, which can also be rationalized with a model of caged atoms [4,7]. The fact that these materials do not show rapid oxidation of the metal also serves as strong circumstantial evidence of the notion of atom encapsulation.

Unfortunately, definitive structural tests, such as X-ray crystallography require material of reasonably high purity. Metallofullerene samples of adequate size and purity are not yet available. One way to circumvent this problem is the use of EXAFS spectroscopy, which utilizes the fine structure observed in X-ray absorption edges to obtain structural information. When an atom absorbs an X-ray, it may eject an electron from its core. Surrounding atoms will then

scatter the outgoing electron wave back upon itself, creating an interference effect. The interference pattern, which manifests itself in the fine structure of the absorption coefficient, depends on the distances, numbers and types of neighboring atoms. Since the radiation can be specifically tuned to the X-ray absorption edge of the metal atom of interest, it is possible to perform such an experiment with relatively dilute samples.

A recent EXAFS study of a sample containing yttrium metallofullerene concluded that the metal is most likely outside of the cage [14]. Here we report EXAFS experiments with material containing yttrium fullerenes, which we performed at a temperature of 10 K as well as at room temperature. Our experimental data can be most satisfactorily interpreted if the yttrium is endohedral, in a position consistent with those found in recent model calculations [12,13].

2. Experimental

Yttrium metallofullerene samples were prepared as described previously [10], except after an initial cold toluene extraction, a cold CS_{82} extraction was used. The resulting powder was analyzed by laser desorption post ionization mass spectrometry as shown in fig. 1 [15]. In addition to bare fullerenes, the measured spectrum at 193 nm shows peaks at the masses of YC_{82} and Y_2C_{82} with about equal intensities. Relative ionization efficiencies of bare fullerenes and metallofullerenes depend on ionization laser fluence. However, based on other experiments, in which we compared mass spectra, taken under similar conditions, with quantitative measurements by XPS and EPR, we believe that fig. 1 gives a reasonable indication of the relative abundances of all the species.

The EXAFS experiment was performed on beamline 7–3 of the Stanford Synchrotron Radiation Laboratory (SSRL) using a Si[220] monochromator crystal. Standard gas ionization chambers were used to measure the incident and transmitted X-ray flux. For the dilute metallofullerenes, the Y absorption was obtained from the X-ray fluorescence, measured using a Lytle fluorescence detector. The photon energy was calibrated by the absorption edge of an yttrium metal foil. Standard compounds of YN and Y_2O_3, were diluted with BN powder. The air sensitive samples were handled in a nitrogen environment.

3. Results

Fig. 2 shows the raw absorption data at 10 K, plotted versus the photon energy. The EXAFS signal $\chi(k)=\mu(E)/\mu_0(E)-1$ in the inset of fig. 1 was obtained from the absorption data by fitting the background, $\mu_0(E)$, to a series of splines through the data and then calculating $\mu(E)/\mu_0(E)$. We limited the upper end of the Fourier transform range to 9 $Å^{-1}$ in K space in order to avoid a monochromator glitch,

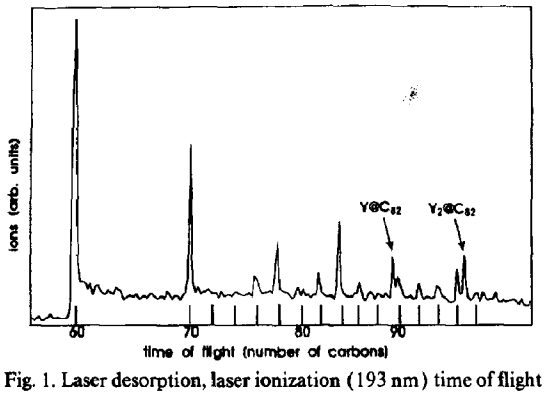

Fig. 1. Laser desorption, laser ionization (193 nm) time of flight mass spectrum of the sample.

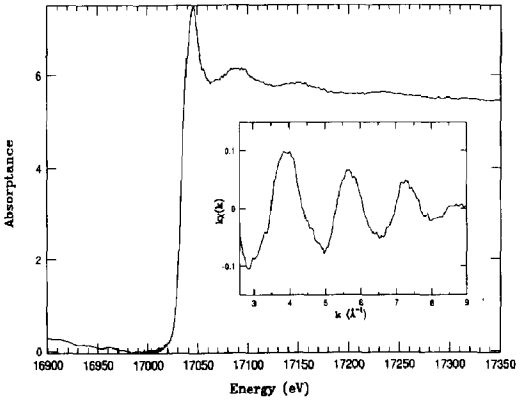

Fig. 2. Raw absorption data at 10 K in energy space. Inset: corresponding k-space transform of the same data.

and the lower end to $K=2.6$ Å^{-1} because of near edge structure. Both ends of the data range are terminated by a Gaussian envelope. The signal appears to be dominated by a damped single frequency, which suggests two conclusions a definite shell exists in the local structure of the yttrium atoms and yttrium is bonded with similar bond lengths to the shell in both the YC_{82} and the Y_2C_{82} species.

The analysis of the EXAFS data was carried out as follows. First, various possible structures of the sample were assumed. For each structural model, a theoretical $\chi(k)$ for each shell was generated by FEFF5, a code for calculating the backscattering amplitude and phase [16]. The same K region and same Gaussian envelope as the experimental data were used. Second, a non-linear fitting code was used to produce the best fit to experimental data by adjusting the following four structural parameters: (i) the number of neighbors, (ii) the interatomic distances (r), (iii) the Debye–Waller factors, (σ), considering both thermal and static disorder, and (iv) the threshold energy (E_0). The FEFF5 calculations have been compared to a large number of isolated pair standards extracted from experimental data collected for standard compounds. The agreement is remarkably good, particularly for Z backscattering atoms. The error in r is less than 0.02 Å for different standard pairs and the amplitude agrees within 15% [17]. The same routine was tested with YN and Y_2O_3 with satisfactory results as well. The quality of fit, R, is expressed as a precentage error per point and depends, among other factors, on the range in r space over which the fits are carried out. Good fits have $R<1\%$.

As a first-order approximation we assumed a single shell of carbon atoms around each yttrium atom and fitted the data over the r space range 1.5–3.0 Å. With this assumption we find that the procedure converges toward a poor fit ($R=2.6\%$) with unrealistic Debye–Waller factors (4×10^{-4} Å versus 6×10^{-2} Å for typical standard compounds). This is not surprising in view of the fact that the EXAFS signal has a structure, indicative of the existence of more than one shell, within a limited range of bond distances. The node at 2.5 Å in fig. 4 can be interpreted as arising from two-shell interference, as will be discussed below. In order to discuss more realistic models, we consider fig. 3, which shows a generic

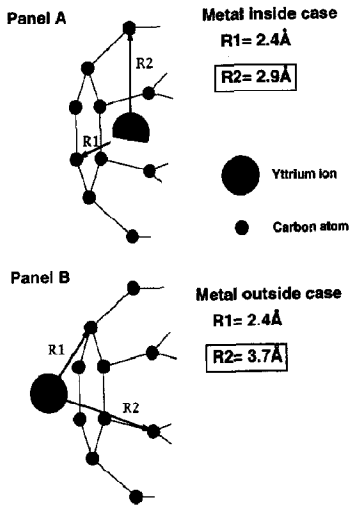

Fig. 3. Panel A and panel B show models of the endohedral and exohedral cases with the distances to the nearest carbon neighbors.

picture of an yttrium atom, endohedral (A) and exohedral (B) to a fullerene cage. In both cases, we positioned the yttrium atom centrally over a hexagon with a distance of 2.4 Å from the first carbon neighbors. Clearly, in either case the number of nearest neighbors in each of the first two shells is 6. However, in the endohedral case, the second shell of 6 carbon atoms is much closer to the first one than in the exohedral case. Assuming a locally spherical curvature of the carbon cage with a diameter of about 8 Å, the second shell would be at 2.9 Å when the metal is inside the cage, whereas it would be at 3.7 Å when the metal is outside the cage. Therefore, as a second-order model, we have simulated the data with the same procedure and the same r-space range, but assuming two shells rather than one. When we choose to set the initial conditions to match the configuration in panel A of fig. 3, the computation converges to the values summarized in table 1 with $R=0.3\%$. This is an improvement of nearly an order of magnitude over the single-shell model, while at the same time the Debye–Waller factors are more realistic. The room temperature data are broader than the 10 K data and have poorer signal to noise, but can still be fit with the same two shells, assuming the same bond lengths and the same numbers of nearest neighbors, with $R=0.8\%$. Fig. 4 compares the resulting simulation with the experimental data at 10

Table 1
Parameters from two shell fit to 10 K data

Shells	Number of carbons ± 1	Distance r in Å ± 0.05	Sigma (σ)	Threshold energy, E_0 (eV)
1st Y–C shell	6	2.40	0.10	2.2
2nd Y–C shell	6	2.85	0.13	2.2

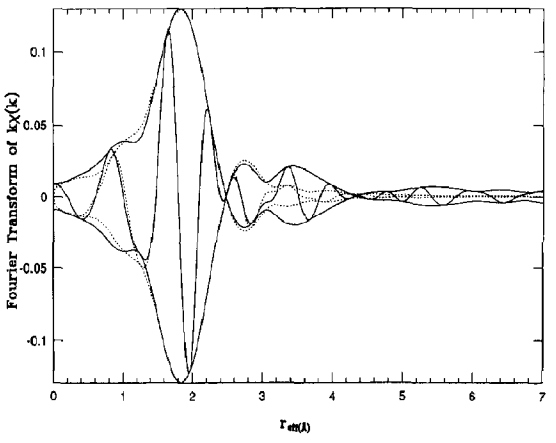

Fig. 4. R space data (solid line) and a fit to the data with an assumed endohedral geometry (dotted line). The fit was calculated with only the first two carbon shells.

K in r space. The wavy line inside the envelope is the real part of the EXAFS signal and the envelope is the amplitude of the EXAFS signal. A good fit must be in good agreement with both the real part and the amplitude. The simulation is consistent with the data up to 3 Å in real space. The experimental signal beyond this distance suggests weak contributions from atoms at somewhat larger distances. This signal is not matched by the calculated spectrum since that is based on a model that only accounts for the first two shells. We have also made an effort to fit the data by assuming a second carbon shell far from the first carbon shell in order to simulate the exohedral case of fig. 3. This produces an unsatisfactory fit with an R value of 1.2% and unrealistic fitting parameters such as a large E_0 shift.

Because the r-space data usually represent a form of radial distribution of neighbor atoms, one might have anticipated a two-shell model to produce two peaks near each other corresponding to the first two shells. However, the fact that we do not resolve two peaks can be understood if we decompose the fit into contributions from individual carbon shells as shown in fig. 5. The real parts of the signals from the two carbon shells are almost out of phase with each other in r space. Their interference is therefore destructive, creating the node that is observed in our data rather than two peaks.

We were also able to successfully simulate the data including the longer r-space region (1.5–4 Å) by introducing two more carbon shells and an yttrium shell. However, the fitting is more complicated and less reliable, because we need to consider multiple scattering effects in the longer r-space range, and we have introduced more fitting parameters.

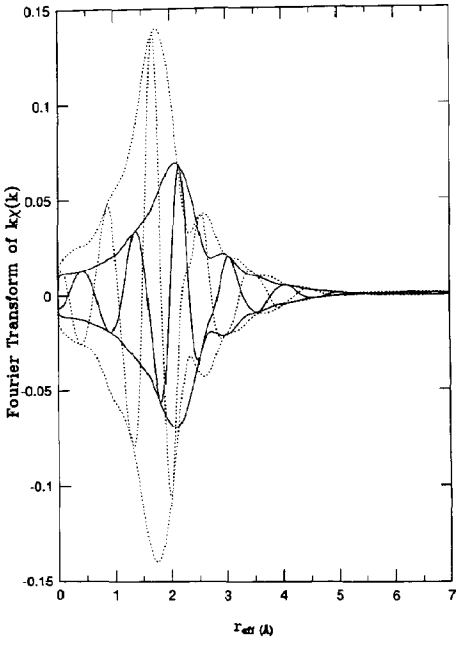

Fig. 5. Decomposition of the fit. The dotted line is the calculated EXAFS signal resulting from the first carbon shell and the solid line is the calculated EXAFS signal resulting from the second carbon shell.

4. Discussion

While our data cannot be deconvoluted to produce a unique structure, it is possible to test specific models, using the procedures outlined above. All theoretical work to date predicts that the lowest energy configuration for metallofullerenes occurs with the metal inside the cage and off center [12,13,18–24]. Two specific models are available from recent calculations. Both Laasonen et al. [12] and Nagase et al. [13] have reported theoretical calculations for LaC_{82}. The former assumed C_{3v} symmetry for the C_{82} cage, while the latter used a cage with C_2 symmetry. Both groups conclude that in its minimum energy position the metal atom is to be inside the cage at about 2.5 Å from the nearest carbons. This is consistent with our experimental findings for yttrium. Nagase et al. place the metal atom under a hexagon, while Laasonen et al. do not. Both models are consistent with our results and cannot be distinguished with our resolution. With our procedure we can only optimize a simulation when definite shells can be assumed. The optimum placement of the metal atom is proposed by Laasonen et al. is asymmetric with respect to all the carbon atoms and therefore does not produce distinct shells. However they do predict 10 nearest neighbors while we find $12 \pm 15\%$.

We can exclude a simple exohedral model, as shown in fig. 3b. A difference of more than 1 Å between the first two shells would certainly be resolved. However, our data are not sufficient to disprove more complex exohedral models, such as one in which an yttrium atom or ion is sandwiched between a C_{82} and another fullerene. In such a case there could be 6 nearest carbons from each cage to contribute to the EXAFS scattering. One argument against such a scenario is that in mass spectrometry the metal is always observed associated with a single C_{82}. Furthermore, a metal atom on the outside of a fullerene cage would be in a different average environment, depending on whether the fullerenes are rotating or not. We know that bare C_{60} molecules rotate readily at room temperature [25–28]. An indication that the same holds true for metallofullerenes can be derived from the observation that the EPR spectra of metallofullerenes (including yttrium fullerenes) in toluene solution broaden dramatically upon cooling below about 180 K [29]. The fact that we do not observe a transition to a different local structure when comparing our room temperature and 10 K data, suggests that one of the following holds: (1) the metallofullerenes do not rotate at room temperature; (2) a complex of two fullerenes sandwiching an yttrium atom is bound sufficiently strongly to move as one molecule at room temperature; or (3) the metal is inside the cage and therefore always sees the same environment, independent of the orientation of the cage itself. The first possibility is unlikely in view of the EPR results, while the second possibility is unlikely in view of the mass spectrometry results. This leaves us with the endohedral model as the most likely explanation for the similarity between our room temperature and 10 K data. The somewhat large Debye–Waller factors derived from the 10 K data indicate static disorder, for which there are several possible explanations. First of all, there may be a multitude of structural isomers, both in terms of different cage structures [8,10] and in terms of different Y positions. It could also be that there are small differences in distances in the Y_2C_{82} and YC_{82} species or the yttrium might be slightly displaced from the centered-over-hexagon position. Large structural differences between the immediate yttrium environments in YC_{82} and Y_2C_{82} are unlikely. There can at most be a few tenths of an angstrom difference in the bond lengths of the two species, since otherwise more shells would be observed. This suggests that in the different isomers, as observed by EPR [8,10], the yttrium atom is always stuck to the side of the cage in a similar position.

Our conclusion that our EXAFS data support the hypothesis that the yttrium atoms are endohedral contrasts with the previous EXAFS study [14]. In that study the authors concluded that the Y atom is exohedral based on a strong double peak seen between 3 to 4 Å, which is not observed in our data. The Fourier back-transformation of that peak shows that it is due to Y–Y scattering. The structure seen in our data for this range of r is much weaker and has distinctly different behavior. This is very contradictory since mass spectra of our sample show abundant Y_2C_{82} while the mass spectra in ref. [14] show none. We note that the double peak seen in the EXAFS data of ref. [14] is identical to the Y–Y peak seen in Y_2O_3, leading us to speculate that there may be Y_2O_3 present in that sample.

5. Summary

EXAFS data obtained from fullerene material, containing both YC_{82} and Y_2C_{82} can be fit with a model with two six carbon shells at 2.4 and 2.9 Å, respectively. Although a unique structure cannot be derived from these data, the results are consistent with a model that places the metal atom off center inside the cage, as predicted in recent theoretical calculations.

Acknowledgement

We would like to thank Tami Westre, Susan Shadle, Dr. B. Hedman and other students of Dr. Hodgson's group for technical help during the experiment. We also want to thank Dr. J. Stohr, Dr. J. Boyce, Dr. J. Rehre, and Dr. M. Hoinkis for very helpful discussions. The EXAFS experiment was carried out at the Stanford Synchrotron Radiation Laboratory which is operated by the DOE Office of Basic Energy Sciences, Division of Chemical Sciences. The Office's Division of Materials Science has provided support for this research.

References

[1] R. Heath, S.C. O'Brien, Q. Zhang, Y. Liu, R.F. Curl, H.W. Kroto, Q. Zhang, F.K. Tittel and R.E. Smalley, J. Am. Chem. Soc. 107 (1985) 7779.

[2] D. Weiss, J.L. Elkind, S.C. O'Brien, R.F. Curl and R.E. Smalley, J. Am. Chem. Soc. 110 (1988) 4464.

[3] R.D. Johnson, M.S. de Vries, J. Salem, D.S. Bethune and C.S. Yannoni, Nature 365 (1992) 239.

[4] C.S. Yannoni, M. Hoinkis, M.S. de Vries, D.S. Bethune, J. Salem, M.S. Crowder and R.D. Johnson, Science 256 (1992) 1191.

[5] H. Weaver, Y. Chai, G.H. Kroll, C. Jin, T.R. Ohno, R.E. Haufler, T. Guo, J.M. Alford, J. Conceicao, L.P.F. Chlbante, A. Jain, G. Palmer and R.E. Smalley, Chem. Phys. Letters 190 (1992) 460.

[6] C.S. Yannoni, H.R. Wendt, M.S. de Vries, R.L. Siemens, J. Salem, J. Lyerla, R.D. Johnson, M. Holnkis, M.S. Crowder, C.A. Brown and D.S. Bethune, Synth. Metals, in press.

[7] H. Shinohara, H. Sato, M. Ohkohchi, Y. Ando, T. Kodama, T. Shida, T. Kato and Y. Salto, Nature 357 (1992) 52.

[8] S. Suzuki, S. Kawata, H. Shiromaru, K. Yamaguchi, K. Kikuchi, T. Kato and Y. Achiba, J. Phys. Chem. 96 (1992) 7159.

[9] H. Shinohara, H. Sato, Y. Saito, M. Ohkohchi and Y. Ando, J. Phys. Chem. 96 (1992) 3571.

[10] M. Hoinkis, C.S. Yannoni, D.S. Bethune, J.R. Salem, R.D. Johnson, M.S. Crowder and M.S. de Vries, Chem. Phys. Letters 198 (1992) 461.

[11] S. Bandow, H. Kitagawa, T. Mitani, H. Inokuchi, Y. Saito, H. Yamaguchi, N. Hayashi, H. Sato and H. Shinohara, J. Phys. Chem. 96 (1993) 9609.

[12] K. Laasonen, W. Andreoni and M. Parrinello, Science 258 (1992) 1916.

[13] S. Nagase, T. Kato and Y. Achiba, Chem. Phys. Letters 201 (1993) 475.

[14] L. Soderholm, P. Wurz, K.R. Lykke, D.H. Parker and F.W. Little, J. Phys. Chem. 96 (1992) 7153.

[15] G. Meijer, M.S. de Vries, H.E. Hunziker and H.R. Wendt, Appl. Phys. B 51 (1990) 395.

[16] J.M. deLeon, J.J. Rehr, S.I. Zabinsky and R.C. Albers, Phys. Rev. B 44 (1991) 4146.

[17] G.G. Li and F. Bridges, to be published.

[18] P.P. Schmidt, B.I. Dunlap and C.T. White, J. Phys. Chem. 95 (1992) 10537.

[19] J.L. Ballester and B.I. Dunlap, Phys. Rev. A 45 (1992) 7985.

[20] B.I. Dunlap, J.L. Ballester and P.P. Schmidt, J. Phys. Chem. 96 (1992) 9781.

[21] A.L. Bug, A. Wilson and J.A. Voth, J. Phys. Chem. 96 (1992) 7864.

[22] G. Cardini, P. Procacci, P.R. Salvi and V. Schettino, Chem. Phys. Letters 200 (1992) 39.

[23] D. Östling and A. Rosen, Chem. Phys. Letters 202 (1993) 389.

[24] Y. Wang, D. Tománek and R.S. Ruoff, Chem. Phys. Letters, 208 (1993) 79.

[25] C.S. Yannoni, R.D. Johnson, G. Meijer, D.S. Bethune and J.R. Salem, J. Phys. Chem. 95 (1991) 9.

[26] R. Tycko, R.C. Haddon, G. Dabbagh, S.H. Glarum, D.C. Douglass and A.M. Mujsce, J. Phys. Chem. 95 (1991) 518.

[27] R. Tycko, G. Dabbagh, R.M. Fleming, R.C. Haddon, A.V. Makhija and S.M. Zahurak, Phys. Rev. Letters 67 (1991) 1886.

[28] R.D. Johnson, C.S. Yannoni, H.C. Dorn, J.R. Salem and D.S. Bethune, Science 255 (1992) 1235.

[29] M. Hoinkis, private communication.